EFFECT OF FAST CURE CYCLES ON MODE I AND MODE II INTERLAMINAR FRACTURE TOUGHNESS FOR INTERLAYER TOUGHENED PREPREG COMPOSITES

Cheng Chen[1], Anoush Poursartip[1], Göran Fernlund[1]
[1]Composites Research Network, Materials Engineering Department, the University of British Columbia,

309-6350 Stores Road

Vancouver, BC Canada V6T 1Z4

ABSTRACT

Faster cure cycles for thermoset prepreg composites are required to achieve higher production rates in the aerospace industry. This work studies the effect of fast cure cycles on the static Mode I (G_{Ic}) and Mode II (G_{IIc}) interlaminar fracture toughness of an interlayer toughened composite material system, T800SC/3900-2B. Composite laminates were processed to the same degree of cure using a manufacturer's recommended cure cycle (MRCC), and three faster cure cycles with high heating rates (>2.8 °C/min) or high curing temperatures (>180 °C). The initiation and propagation G_{Ic} and G_{IIc} were measured using Double Cantilever Beam (DCB) and End-notched Flexure (ENF) tests under static loading, respectively. Results show that curing conditions affect interlayer microstructures and the morphology of toughening particles. However, the initiation and propagation G_{Ic} and G_{IIc} are not sensitive to the applied higher heating rates and curing temperatures. These results suggest that there may be an opportunity to greatly reduce the processing time for T800SC/3900-2B prepregs using faster cure cycles outside of the manufacturer's recommended processing window, yet retaining high interlaminar fracture toughness.

Keywords: Polymer-matrix composites (PMCs), Particle-reinforced composites, Delamination, Fracture toughness
Corresponding author: Göran Fernlund

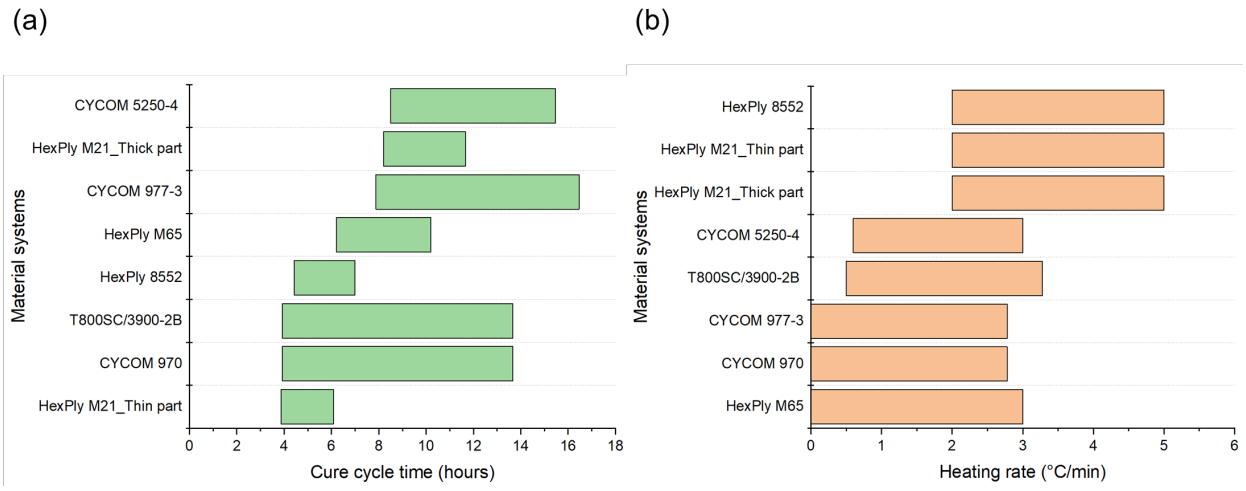
1. INTRODUCTION

Increasing production rates of carbon fibre structures in commercial airplanes is crucial to meet market needs. Carbon fibre reinforced thermoset composites have been widely used to manufacture primary structures of commercial airplanes such as wings and fuselage. Significant effort has been made to accelerate the manufacturing process for aerospace composite parts using automated composite layup machinery such as automated fibre placement (AFP) and automated tape-laying (ATL). However, the production rate is still limited by the manufacturer's recommended cure cycles (MRCC) for aerospace-grade thermoset prepreg composites. Figure.1

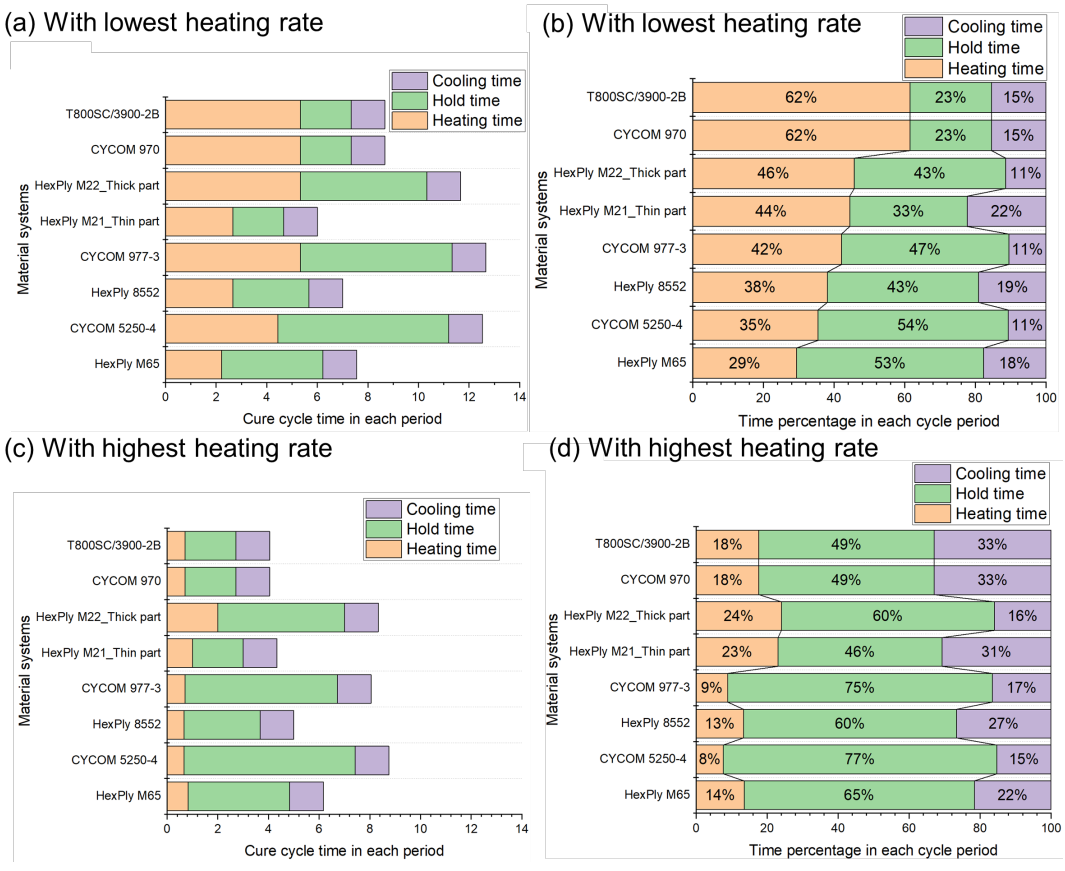
Copyright 2020. Used by the Society of the Advancement of Material and Process Engineering with permission.

(a) shows that the MRCC usually lasts for 4-16 hours to complete cure and achieve high quality [1–7]. One of the solutions to shorten the cure cycle time is to redesign the resin chemistry. There are many signs of progress in developing and commercializing fast-cure resin systems for high high-volume production in the automotive industry [8,9]. For the aerospace industry, however, due to the high certification cost for a new material system, it is desirable to develop a faster cure cycle for a mature material system that has already been certified for aerospace applications. The material manufacturer usually provides a conservative processing window for its composite material product. Figure.1 (b) shows recommended cure cycle heating rates for thermoset prepreg composite material that are being used for airplane structures. The maximum allowed heating rates for these material systems are usually lower than 5 °C/min. Figure. 2 shows the cure cycle time and the proportion for each stage of the cure cycle using the lowest and highest recommended heating rates for different aerospace thermoset composites. Using the highest heating rates, the cure cycle time is limited by both the heating stage (29-62%) and holding stage (23-53%), as shown in Figure.2 (a-b). Figure.2 (c-d) suggests that the cure cycle time is dominated by the holding stage at 180 °C using the highest recommended heating rates. To shorten the cure cycle time, a faster cure cycle with a higher heating rate and a higher curing temperature may improve the manufacturing efficiency and achieve the same quality without significant change to the existing manufacturing process. However, the question remains whether using fast cure cycles outside of the manufacturer's recommended processing window can retain the final physical and mechanical properties. Commercial interlayer toughened prepreg composites such as Toray's T800SC/3900-2B and Hexcel's HexPly® M21E/IMA were chosen for primary structures of commercial airplanes due to their high delamination and damage resistance [10,11]. Thermoplastic particles in the interlayer and thermoplastic-modified thermoset epoxy introduce more complicated compositions and laminate microstructures for toughened material systems, which may make them more sensitive to curing conditions than non-interlayer toughened material systems. Hunt et al. [12] examined various non-standard cure cycles for HexPly® M21E/IMA and found that the Mode I interlaminar fracture toughness (G_{Ic}) and crack propagation behaviours are dependent on curing conditions. Specimens cured with one-hold cure cycles generally exhibit stick-slip behaviours while specimens cured with two-stage cures cycles show stable crack propagation with a 22% reduction of propagation G_{Ic}. For laminates cured with elevated temperature above 180 °C, the crack tends to migrate from the toughened interlayer to the intralaminar region. Incerti et al. [13] found that the fracture toughness of core-shell rubber (CSR) nano-modified epoxies decreases with increasing curing temperature and that this dependence is more significant for epoxies with higher CSR particle weight fractions, which indicates that the dependence is caused by CSR.

This work studies the effect of fast cure cycles with a high heating rate or a high curing temperature on the static Mode I and Mode II interlaminar fracture toughness of T800SC/3900-2B. Laminates were processed to the same degree of cure (DoC=0.9) using the MRCC and non-standard fast cure cycles. G_{Ic} toughness was measured using Double Cantilever Beam (DCB) tests. Initiation and propagation G_{IIc} toughness were measured using non-precracked (NPC) and precracked (PC) end-notched flexure (ENF) tests, respectively. The laminate microstructure was investigated using an optical microscope. The fracture morphology was examined using scanning electron microscope (SEM). This work suggests that there may be a larger processing window for T800SC/3900-2B than the currently suggested one.



Figureure.1. Cure cycle time and recommended heating rates for different aerospace-grade thermoset prepreg composites [1–7].



Figureure.2. Processing time and the proportion of time spent at each stage of the cure cycle using lowest and highest recommended heating rates for different aerospace-grade thermoset composites [1–7].

2. EXPERIMENTATION

2.1 Material and sample preparation

An interlayer toughened prepreg, Toray T800SC/3900-2B unidirectional (UD) tape, was used in this study. In this material system, thermoplastic particles are distributed in the interlayer to improve delamination and impact damage resistance. This material system has been widely used in the primary structures of Boeing's commercial airplanes. All laminates with stacking sequence $[0]_{20}$ were manufactured by hand lay-up on a flat aluminum tool with a non-adhesive film at the laminate-tool interface. A 12.5 μm thick FEP film was inserted at the laminate mid-plane during the layup process as a delamination initiator. The initial delamination length, a_0, was approximately 50 mm for DCB specimens and 45 mm for ENF specimens. Rubber dams were placed around laminates to prevent resin bleed. A flat aluminum plate was placed on top of the laminates to obtain a smooth top surface. After debulking under full vacuum at 23 °C for 12 hours, laminates were cured in an autoclave with 85 psi autoclave pressure. Full vacuum was applied under the vacuum bag throughout the cure cycle. Cure cycles with different heating rates and cure temperatures were used to achieve the same final Degree of Cure (DoC=0.90), as shown in Table.1. The final DoC was calculated with an open cure kinetics model [14] exercised using the Raven process simulation software from Convergent Manufacturing Technologies. After cure, DCB specimens with dimensions of 125 mm (length) × 25 mm (width) × 3.86 mm (thickness) and ENF specimens with dimensions of 130 mm (length) × 25 mm (width) × 3.86 mm (thickness) were cut from large laminate panels using a water-lubricated precision diamond saw (Isomet 400). After that, specimens were conditioned in the standard laboratory atmosphere for seven days.

Table 1. Temperature cure cycles

Type of cure cycle	**MRCC**	**High heating rate**	**High cure temperature**	**High heating rate and curing temperature**
Cure cycle ID	CC1	CC2	CC3	CC4
Heating rate (°C/min)	1.0	7.0	1.0	7.0
Hold temperature (°C)	180	180	200	200
Hold time (min)	110	135	30	40
Cool-down rate (°C/min)	2.78 (same for all)			
Final DoC	0.9 (same for all)			
Total cure cycle time (min)	328	200	275	131
Gel temperature (°C)	173	180	173	200

2.2 Double Cantilever Beam (DCB) test

Double Cantilever Beam test was performed using a universal mechanical testing machine (Instron 5982 Floor Model Testing Systems) following the ASTM 5528-13 standard [15]. Piano hinges were bonded to the specimen using an epoxy adhesive to apply the crack-opening load perpendicular to the debonding plane. The loading rate was 2 mm/min. Five repeats were conducted for each cure cycle. A camera was used to monitor the delamination growth, a. The load (P), load point displacement (δ) and delamination length were recorded simultaneously and used to calculate the strain energy release rate, G_{Ic}. To account for the rotation effect, G_{Ic} was calculated using the Modified Beam Theory (MBT) method by the following equation:

$$G_{Ic} = \frac{3P\delta}{2b(a + |\Delta|)} \tag{1}$$

where Δ is determined experimentally by generating a least square plot of the cube root of compliance, $C^{1/3}$, versus delamination length. b, is the average width of the specimen.

2.3 Quasi-static end-notched flexure (ENF) test

Quasi-static end-notched flexure (ENF) tests were performed using a universal mechanical testing machine (Instron 5982 Floor Model Testing Systems) with a three-point bending fixture according to the ASTM D7905M–14 standard [16], as shown in Figure.1 (a). Five repeats were conducted for each cure cycle. The crosshead loading rate was 0.5 mm/min. Both Non-Precracked (NPC) and Precracked (PC) fracture tests were performed to measure the initiation and propagation G_{IIc}, respectively. NPC tests performed with the 12.5 µm FEP insert as the initial crack. After the crack had grown, a PC test was performed on the same specimen. Two Compliance Calibration (CC) tests were performed at crack lengths of 20 mm and 40 mm, respectively. The CC coefficients, A and m, were determined using a linear least-squares regression analysis of the compliance, C, versus crack length, a, according to the relationship: $\mathrm{C} = \mathrm{A} + \mathrm{m}a^3$. G_{IIc} was then calculated using the following equation:

$$G_{IIc} = \frac{3mP_{Max}^2 a_0^2}{2B} \tag{2}$$

where m is the CC coefficient, P_{Max} is the maximum force from the fracture test, a_0 is the crack length used in the fracture test (30 mm), and B is the specimen width.

2.4 Fractographic analysis

The microstructure of cured laminates was examined from polished 20-ply laminates using an optical microscope (Nikon Eclipse MA200). A scanning electron microscope (FEI Quanta 650, 5 kV) was used to analyze the fracture morphology of the fracture surface of the DCB specimens.

3. RESULTS

3.1 Interlayer microstructure

Thermoplastic particles are introduced to the interlayer of T800SC/3900-2B laminates to improve delamination and impact resistance. The interlayer topology such as particle volume fraction in the interlayer and interlayer thickness impacts the toughening effect. Therefore, it is of great interest to examine whether the interlayer topology is influenced by curing conditions. Figure.3 shows the interlayer microstructure of T800SC/3900-2B laminates processed using a standard cure cycle (CC1) and faster cure cycles (CC2, CC3 and CC4). For the standard cure cycle CC1, particles deform slightly and contact fibres and adjacent particles. The interlayer microstructure for CC3 with a higher curing temperature of 200 °C and a standard heating rate of 1.0 °C/min is similar to that of CC1. Compared to CC1 and CC3, the particle deformation is larger for CC2 with a higher heating rate of 7.0 °C/min and a standard curing temperature of 180 °C. For CC4 with a higher heating rate of 7 °C/min and a higher curing temperature of 200 °C, particles deform significantly and are highly compacted. The interlayer for CC4 is thinner than those for CC1-CC3. Causes of particle deformation and interlayer thinning have been revealed in previous work [17]. Generally, if the gelation temperature of the base resin is lower than the glass transition temperature of thermoplastic particles ($T_g^p = 150$ °C), particles cannot deform due to the constraining effect of gelled resin. On the other hand, If the gelation temperature of the base resin is higher than T_g^p, particles will deform under the fibre bed pressure when the resin is still fluid, which results in interlayer thinning. Table.1 shows that the gel temperature for CC1 and CC3 is the same, which causes similar microstructures for both cure cycles. The gel temperature is 180 °C for CC2 and 200 °C for CC4, which are higher than T_g^p and gel temperatures for CC1 and CC3. Therefore, particle deformation for CC2 and CC4 is larger than CC1 and CC3.

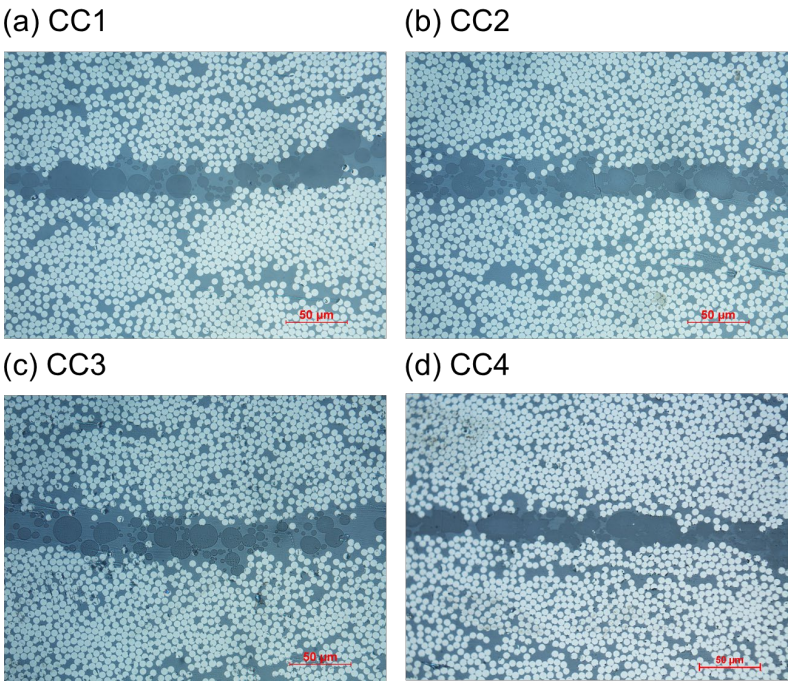


Figure.3. The interlayer microstructure of T800SC/3900-2B processed using different cure cycles

3.2 Mode I Interlaminar fracture toughness

A typical delamination resistance curve (R-curve) for the DCB samples is displayed in Figure.4. Unstable crack growth occurs after the crack initiation from the preimplanted insert and is arrested after. The initial propagation G_{Ic} is lower than initiation G_{Ic} due to loss of the toughening effect. After the crack arrests, propagation G_{Ic} increases as the crack grows due to increasing fibre bridging and finally reaches a plateau. Therefore, the saturated propagation G_{Ic} is higher than the initial propagation G_{Ic}. Figure.5. compares the initial G_{Ic}, initial propagation G_{Ic}, and saturated propagation G_{Ic} for different cure cycles. The initial G_{Ic} for CC2, CC3 and CC4 is slightly higher than that for the standard cure cycle CC1. The initial propagation G_{Ic} and saturated propagation G_{Ic} are not sensitive to curing conditions. The measured initiation G_{Ic} value may be influenced by the shape and quality of crack tip made by the preimplanted insert. Figure.6 shows the fracture morphology for different cure cycles under Mode I loading. The result shows that the crack goes through particles and that particle-resin debonding is not observed, which indicates high particle-resin interfacial strength. Particles processed using CC1 and CC3 have a uniform internal microstructure. However, for CC2 and CC4 with a higher heating rate, particles have a core-shell microstructure. These results show that curing conditions affect the particle morphology and may influence the properties of toughening particles.

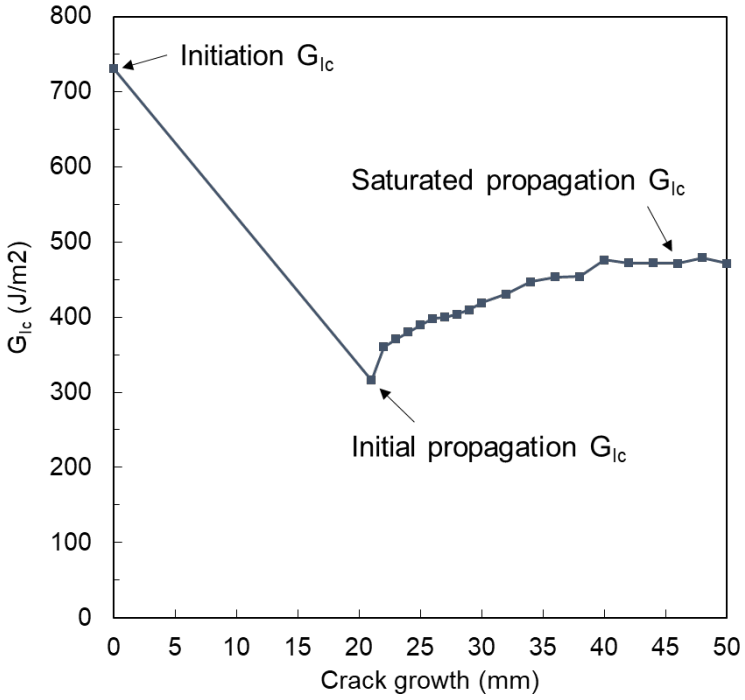


Figure.4. Determination of initial G_{Ic}, initial propagation G_{Ic}, and saturated propagation G_{Ic}.

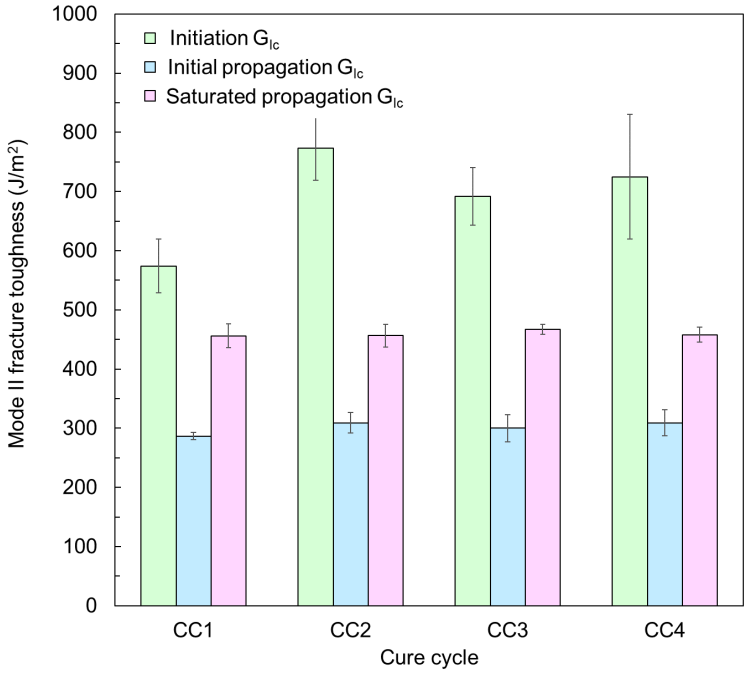


Figure.5. The initial G_{Ic}, initial propagation G_{Ic}, and saturated propagation G_{Ic} at different cure cycles.

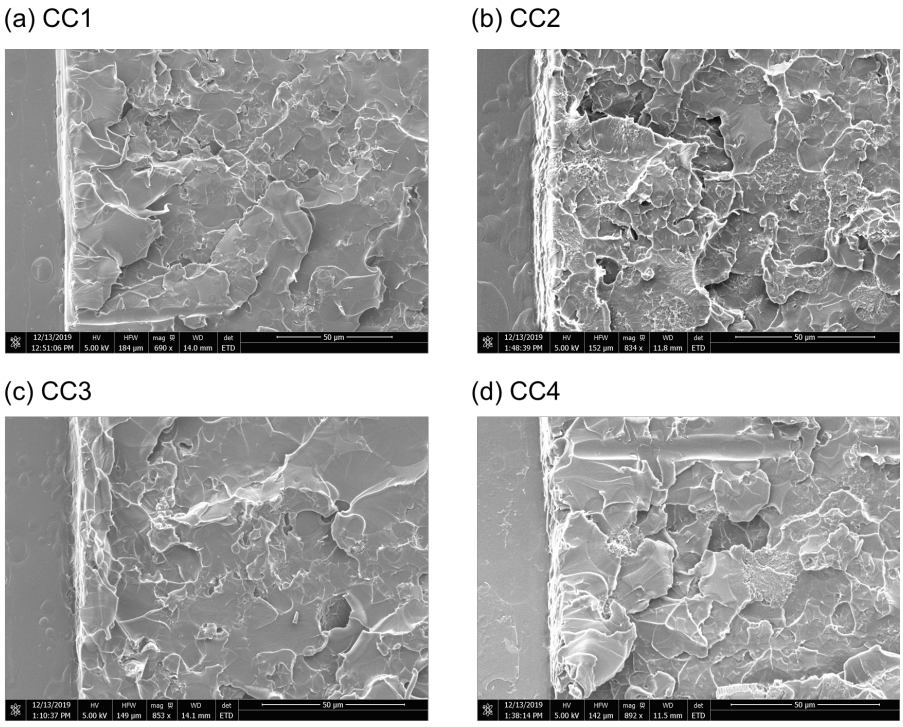


Figure.6. Mode I fracture morphology at different cure cycles.

3.3 Mode II Interlaminar fracture toughness

Figure.7 compares initial and propagation G_{IIc} for different cure cycles. The initiation G_{IIc} was measured from the preimplanted insert, and the first and second propagation G_{IIc} were measured at a distance away from the preimplanted insert. There is a minor difference in initiation and propagation G_{IIc} between these four cure cycles. Interestingly, G_{IIc} decreases slightly as the crack grows, which is due to the crack migration from toughened interlayer to more brittle intralayer, as shown in Figure.8. It has been reported that the rate of crack migration to the intralayer is determined by the curing condition and strain rate [18]. It was found that the rate of crack migration is high for cure cycles with either low heating rate or low curing temperature, which results in a significant reduction of G_{IIc} during crack propagation. For the standard cure cycle and the faster cure cycles used, most of the crack remains in the toughened interlayer during crack propagation. It is desirable to maintain the crack within the interlayer or at the boundary of interlayer to keep the toughening effect such as interlayer plastic deformation. Compared to the standard cure cycle CC1, the cure cycle time for CC2, CC3 and CC4 is reduced significantly while initiation and propagation G_{IIc} are retained.

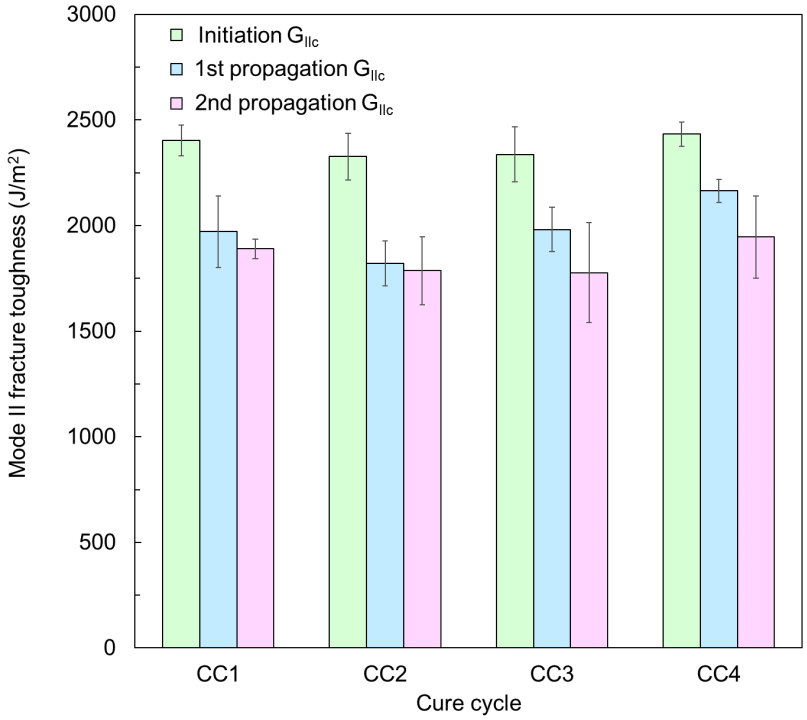


Figure.7. The initial and propagation G_{IIc} at different cure cycles.

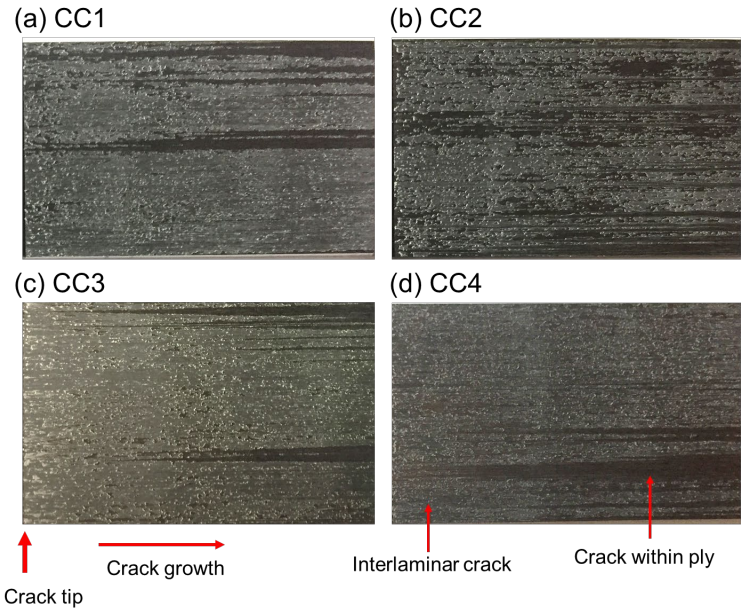


Figure.8. The fracture surface of the bottom side of ENF specimens for at different cure cycles.

4. CONCLUSIONS

This work examined the effect of fast cure cycles on the interlayer microstructure and the quasi-static G_{Ic} and G_{IIc} of T800SC/3900-2B. It was found that not only interlayer microstructures such as interlayer thickness and particle shape but also the particle internal morphology are influenced by curing parameters such as heating rate and curing temperature. Fast cure cycles with higher heating rates or curing temperatures do not affect propagation G_{Ic} but may improve initial G_{Ic}. The results of ENF tests showed that G_{IIc} decreases as the crack grows for all cure cycles, which is a results of local crack migration from the toughened interlayer to the more brittle intralayer. Initiation and propagation G_{IIc} are not sensitive to curing conditions. There have been concerns raised about the negative effect of fast cure cycles on the interlaminar fracture toughness of interlayer toughened composites. This work indicates that higher heating rates and higher curing temperatures outside of the recommended cure cycle do not reduce interlaminar fracture toughness of T800SC/3900-2B. Therefore, there may be a larger processing window for T800SC/3900-2B prepregs than what is currently used. More cure cycles and properties should be exzamined to establish the true processing window for T800SC/3900-2B prepregs in the future.

5. ACKNOWLEDGEMENTS

The authors declare no conflict of interest. This research was financially supported by the Composites Research Network (CRN). We would also like to thank the Boeing Company and Convergent Manufacturing Technologies for their support. The authors acknowledge Dr. Karl M. Nelson and Pete George from the Boeing Company for providing insight and guidance in this research.

6. REFERENCES

[1] Inc. TCMA. 3900 PREPREG SYSTEM Catalogue 2017.

[2] Hexcel. HexPly ® M21 - Product Data Sheet - EU Version. Hexcel 2015.

[3] Cytec Industries. CYCOM ® 5250-4 Technical Data Sheet 2011.

[4] Cytec Industries. 977-3 Epoxy Resin System 2006.

[5] HEXCEL. HexPly ® M65 Product Data Sheet. 2016.

[6] Hexcel. HexPly 8552 Product Data Sheet 2016:1–6.

[7] Cytec Industries Inc. AEROSPACE MATERIALS CYCOM ® 970 Epoxy Resin. 2013.

[8] SLOAN PM& J. Fast and Faster: Rapid-cure resins drive down cycle times. CompositesWorld 2018. https://www.compositesworld.com/articles/fast-and-faster-rapid-cure-epoxies-drive-down-cycle-times.

[9] Nguyen FN, Yoshioka K, Toshiya Kamae IT, Kitano A. Fast-cycle cfrp manufacturing technologies for automobile applications n.d.

[10] Odagiri N, Kishi H, Yamashita M. Development of torayca prepreg p2302 carbon fiber reinforced plastic for aircraft primary structural materials. Adv Compos Mater 1996;5:249–54. doi:10.1163/156855196X00301.

[11] Hexcel. Hexcel ready to fly on the A350 XWB. Reinf Plast 2013;57:25–6. doi:10.1016/s0034-3617(13)70089-4.

[12] Hunt C, Kratz J, Partridge IK. Cure path dependency of mode i fracture toughness in thermoplastic particle interleaf toughened prepreg laminates. Compos Part A Appl Sci Manuf 2016;87:109–14. doi:10.1016/j.compositesa.2016.04.016.

[13] Incerti D, Wang T, Carolan D, Fergusson A. Curing rate effects on the toughness of epoxy polymers. Polymer (Guildf) 2018;159:116–23. doi:10.1016/j.polymer.2018.11.008.

[14] Donna Dykeman. Minimizing uncertainty in cure modeling for composites manufacturing. University of British Columbia, 2008. doi:10.14288/1.0066334.

[15] ASTM D5528-01. Standard test method for mode I interlaminar fracture toughness of unidirectional fiber-reinforced polymer matrix composites. Am Stand Test Methods 2014;03:1–12. doi:10.1520/D5528-13.2.

[16] ASTM D7905. Standard test method for determination of the mode II interlaminar fracture toughness of unidirectional fiber-reinforced polymer matrix composites. Astm 2014:1–18. doi:10.1520/D7905.

[17] Chen C, Poursartip A, Fernlund G. Cure-dependent microstructures and their effect on elastic properties of interlayer toughened thermoset composites 2019. Manuscript submitted for publication.

[18] Chen C, Nesbitt S, Reiner J, Poursartip A, Vaziri R. Cure path dependency of static and dynamic Mode II interlaminar fracture toughness of interlayer toughened composite laminates 2020. Manuscript submitted for publication.